9th INTERNATIONAL CONFERENCE on MATERIALS ENGINEERING and METALLURGY
ONLINE
TEHRAN - IRAN
NOVEMBER 10-11 , 2020
iMat 2020
نهمین کنفرانس بین‌المللی مهندسی مواد و متالورژی
تهران – ایران
۲۰ و ۲۱ آبانماه ۱۳۹۹
و چهاردهمین کنفرانس مشترک
انجمن مهندسی متالورژی و مواد ایران و انجمن علمی ریخته‌گری ایران
بیست و چهارمین کنگره سالانه انجمن مهندسین متالورژی ایران

The effect of anodization temperature of nitinol alloy on the morphology of surface nanoporous layer

Ali Moshfeghi[1], Farshad Davoodian[2], Alireza Mousavi[3], Erfan Salahinejad[4]

Moshfeghiali.am@gmail.com

Abstract

Fabrication of nanostructures through anodization is a promising process as the technique enables easy and low-cost surface modification of metallic substrates with a high degree of control on the resulted nanostructure morphology. In this work, NiTi alloy (nitinol) was anodized in an organic-based electrolyte containing water and Cl^- ions under different anodization temperatures with the aim of investigating the effect of the electrolyte temperature on the morphology and geometry of the obtained nanopores (NPs). According to electron microscopy and statistical analyses, by increasing the anodization temperature, the thickness of the obtained NP layer and the number of formed NPs are decreased, whereas their mean diameter is increased. It is concluded that anodization at room temperature results in the highest obtainable thickness for the NP layer, whereas the samples anodized at 40°C show the highest uniformity in regard to the NP layer thickness and the total number of the formed NPs. Meanwhile, anodization at temperatures around and beyond 80°C results in total destruction of the NP layer. The variations are explained by the dependency of the electrolyte viscosity and thereby the dissolution rate of the anodically-grown oxide layer on the anodization temperature.

Keywords: Nickel-titanium alloy; Electrochemical deposition; Nanopores; Oxidation and dissolution reactions

[1] B.Sc. Graduate, Faculty of Materials Science and Engineering, K. N. Toosi University of Technology, Iran

[2] M.Sc. Graduate, Faculty of Materials Science and Engineering, K. N. Toosi University of Technology, Iran

[3] B.Sc. Graduate, Faculty of Materials Science and Engineering, K. N. Toosi University of Technology, Iran

[4] Associate Professor, Faculty of Materials Science and Engineering, K. N. Toosi University of Technology, Tehran, Iran

1- Introduction

Recently, there has been a trend in utilizing of anodization as a low cost and scalable process for formation of novel nanostructures with high specific surface areas on different alloys [1]. An example of such anodically grown nanostructures is Ni-Ti-O nanoporous oxides which have found applications in electrocatalysis [2, 3], biosensing [4], gas sensing [5], and biomedical engineering [6, 7]. Alongside nanoporous oxides, Ni-Ti-O nanotubes (NTs) are used in many of the aforesaid applications because of their unique combination of physical properties which could offer a better efficiency due to their higher specific surface areas [8]. Nevertheless, further increases in the specific surface area of this nanostructure is not possible because of the restrictions on the maximum obtainable thickness of Ni-Ti-O NTs in the conventional electrolytes. Recent works have shown that the anodic fabrication of Ni-Ti-O NTs on NiTi alloy is morphologically limited to approximately 1 μm of thickness in fluoride-containing electrolytes [9]. Studies on this subject have illustrated that the rapid dissolution of nickel oxides in the electrolytes causes this limitation, which leads to relatively short Ni-Ti-O NTs compared to pure anodically-grown TiO_2 nanostructures on Ti substrates [10].

Anodizing can be used for fabrication of nanopores (NPs) on NiTi alloy which does not suffer from the aforementioned thickness limitation in comparison to NTs. With the purpose of obtaining Ni-Ti-O NPs with higher thickness and higher specific surface area, numerous anodization experiments have been conducted on NiTi with different compositions of organic-based electrolytes, all containing small amounts of H_2O and differing in their etchant constituents: NaCl [11], HCl [12], NaBr [11], and Na_2CO_3 [13]. In a pertinent study, HCl-containing organic electrolytes were used for formation of NPs with a thickness of around 160 μm, successfully increasing the surface area of the nanostructures. In addition to HCl, NaCl-containing electrolytes also provide the formation of thick NP layers on the NiTi substrate.

In the past years, the different parameters of the anodization process of NiTi for the formation of Ni-Ti-O NPs were studied. Hang et al. [14] investigated the influence of anodization time on this process and demonstrated that there is a linear relationship between the anodization duration and NP thickness up to a certain point in time. The influence of electrolyte pH has also been studied by Hang et al [15]. Another important parameter was the post-annealing temperature investigated by Liu et al [16]. In addition, the effect of voltage and time and also electrolyte stirring on the formation of Ni-Ti-O NPs has been reported by Strnad [17] and Zhao [18], respectively.

One of the important parameters in the anodic growth of NPs on NiTi is the electrolyte temperature, which has not been systematically investigated yet. The anodization temperature could have an effect on the electrolyte viscosity and therefore the mobility of the participating ions in chemical reactions that cause the formation of the NP layer. As a result, the morphological properties and the thickness of oxide layer may be affected by changes in the electrolyte temperature. In the present work, the influence of anodization temperature in a NaCl-containing organic electrolyte was investigated to assess how this change affect the resulted nanostructures. For this purpose, the samples were anodized in four different temperatures (room temperature, 40, 60 and 80°C). Subsequently, the achieved NPs were investigated by electron microscopic and statistical analyses.

2- Experimental

The anodization electrolyte was prepared using ethylene glycol (Reag. USP grade, Merck, Germany), sodium chloride (%99.5<NaCl, Merck, Germany) and double-distilled water (purity: 99%, conductivity: 1 $\mu s \cdot cm^{-1}$). NiTi alloy disks (Ni-50Ti, Kellogg's Research Labs, USA) of 9 mm in diameter and 2 mm in thickness were used as the substrates.
Each sample was anodized in 100 ml of an electrolyte containing ethylene glycol, 5 wt% double-distilled water and 0.03 mol NaCl, based on the formulation of Ref. [11]. For the bias voltage of anodization, a DC power supply was used to provide the voltage of 10 V between the working electrode and a 20 mm distanced Pt cathode sheet during anodization. The NiTi disks were ground by abrasive papers, polished to a mirror finish, and then ultrasonicated in a bath of ethanol and distilled water. The non-working side of the disks was connected to a copper wire and then sealed to avoid any contact with the electrolyte. For each anodization temperature, a bath of water with the desired temperature was prepared. The beaker containing the anodization setup was placed in the bath and a thermometer was used in the beaker for temperature monitoring during the process. To investigate the effect of the anodizing temperature on the nanostructure of NPs, four samples were anodized at different temperatures (room temperature, 40, 60 and 80 °C) for the constant duration of 30 min.
To assess the morphology of NPs, field-emission scanning electron microscopy (FESEM, TESCAN, MIRA 3, accelerating voltage= 15 kV) after gold sputtering was used. The analyses were conducted on the as-anodized surfaces and cross-sections of the samples. The ImageJ software was also used for the statistical analysis of the obtained nanostructures.

3- Result and discussion

The formation of NPs in the anodizing process on the NiTi substrate occurs by a balance between two sets of chemical reactions. Oxide reactions make an oxide layer on the NiTi substrate and dissolution reactions that etch the oxide layer. For Cl-containing electrolytes, the following reactions have been reported in the anodization process [8, 19]:

$$Ti + 2H_2O \rightarrow TiO_2 + 4H^+ + 4e^- \quad (1)$$

$$Ni + H_2O \rightarrow NiO + 2H^+ + 2e^- \quad (2)$$

$$TiO_2 + 4H^+ + 6Cl^- \rightarrow [TiCl_6]^{2-} + 2H_2O \quad (3)$$

$$NiO + 2H^+ + 4Cl^- \rightarrow [TiCl_4]^{2-} + H_2O \quad (4)$$

The first and second reactions are the oxidation process and third and fourth reactions are the dissolution reactions.

Fig. 1 shows the surface and cross-section micrographs of the samples anodized in the voltage of 10 V. Fig. 1(a) illustrates that the sample anodized at room temperature are covered by NPs. Fig 1(b) shows the cross-section micrograph of the sample anodized at room temperature, reflecting that the oxide layer on the sample is uniform. Fig. 2 compares the NP layer thickness of the different samples. Evidently, the highest thickness is obtained in the sample which was anodized at room temperature (13.7 μm). It is also shown that by increasing the anodization temperature, the NP layer thickness is lowered, and finally in the sample anodized at 80°C the NP layer is completely destructed. These findings imply that the dissolution of Ni-Ti-O NP layer is intensified by increasing the electrolyte temperature, which is consistent with previous reports on anodically grown Ni-Ti-O NT on NiTi [10]. This can be attributed to the increased mobility of Cl^- ions at higher temperatures as the viscosity of the electrolyte is decreased. The standard deviation (SD) of the thickness also hints at the uniformity of the formed nanoporous oxide layer. By the same token, having the minimum SD value for the 40°C anodized sample, it can be concluded that this sample has the highest uniformity in regards to the NP layer thickness. As it can be seen, in the samples anodized at 60°C the SD value of the obtained thickness is increased compared to the samples anodized at room temperature and 40°C, hinting at lower uniformity.

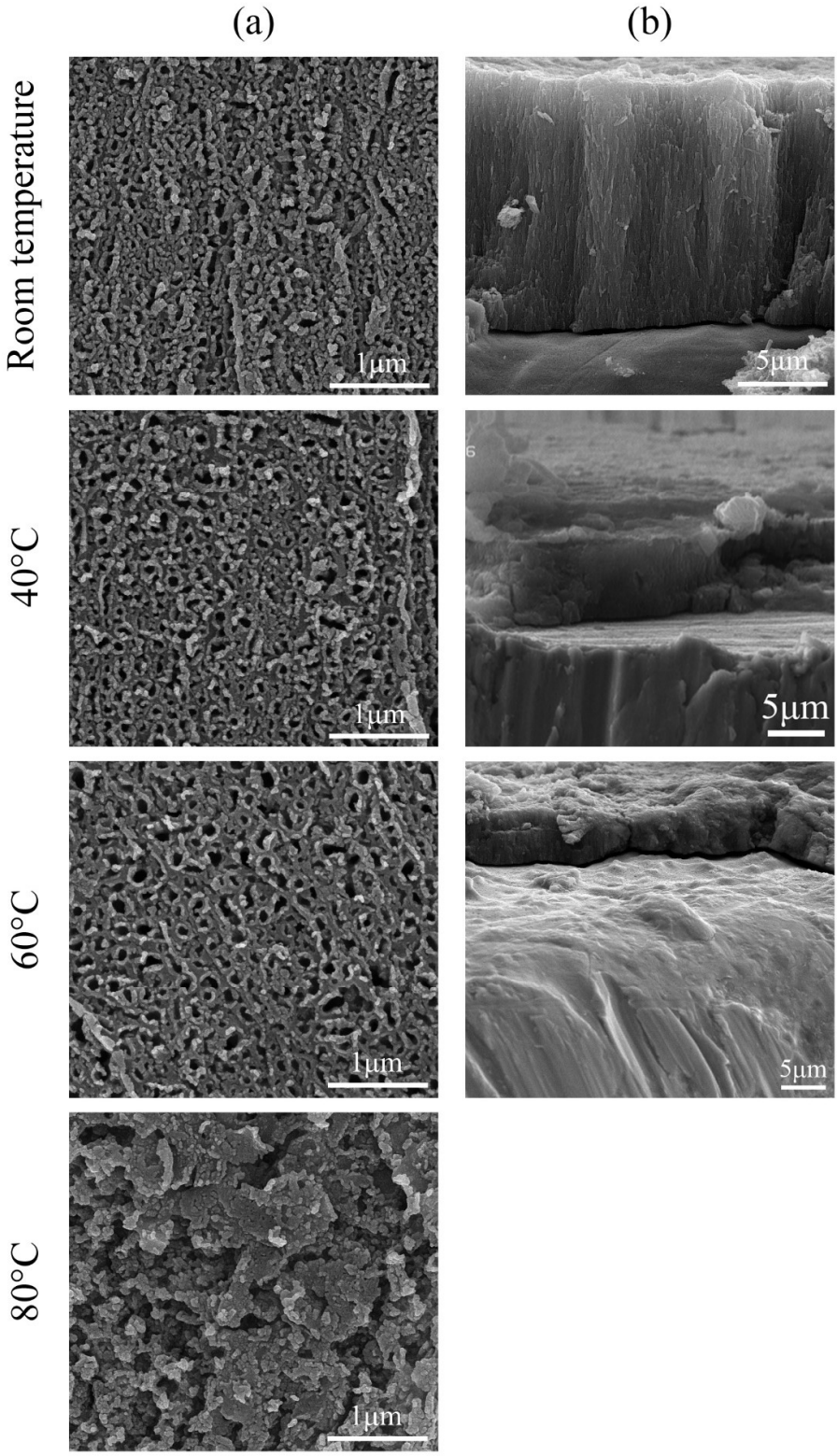

Fig. 1. (a) Surface and (b) cross-sectional FESEM images of the samples.

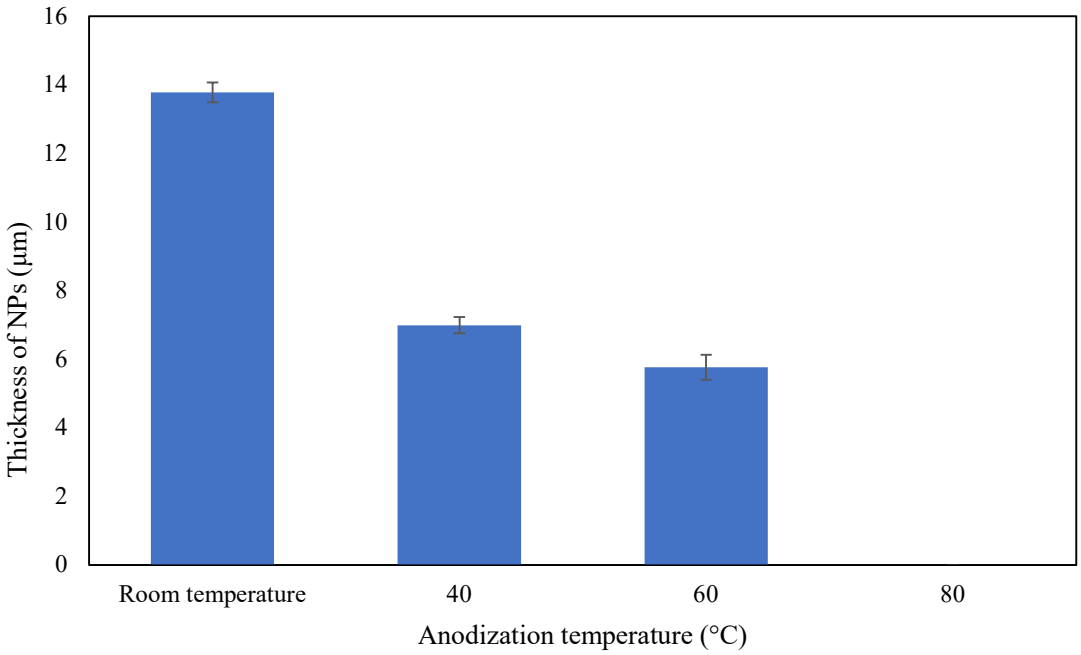

Fig. 2. Cross-sectional thickness of the NP layers grown on the different samples.

Fig. (3) illustrates the diameter of the NPs anodically grown at different temperatures. This data is extracted from the surface micrographs (Fig. 1). Obviously, the increase of the anodization temperature has resulted in the increase of the mean dimeters of NPs. This could also be a result of increasing the ions mobility and therefore dissolution rate. It can be also seen that the SD value for the NP diameters is at high levels for all samples, implying at a scattered distribution of the NP diameters.

Fig. 4 illustrate the NPs diameter distribution on the samples anodized at different temperatures. As it can be seen, the diameter distribution for all samples is widely scattered. This data explains the high value of SD for the NPs diameters. Additionally, it is realized from this diagram that with increase in the temperature of the anodization process, the percentage of NPs with the higher value of diameter is increased. This result is completely in agreement with the mean values of the NP diameters.

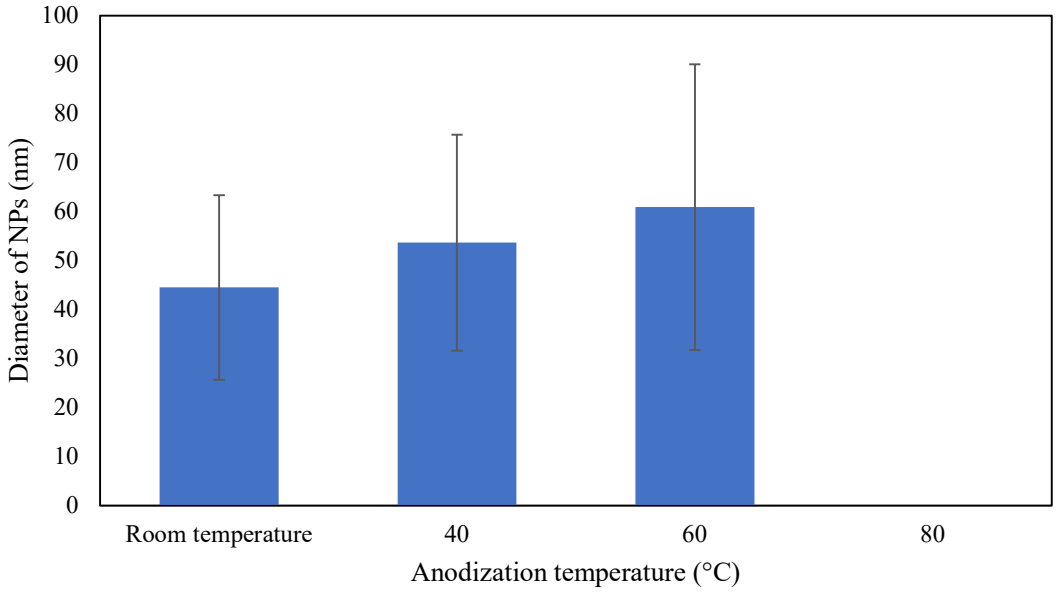

Fig. 3. Diameter of NPs anodically fabricated under the different anodization temperatures.

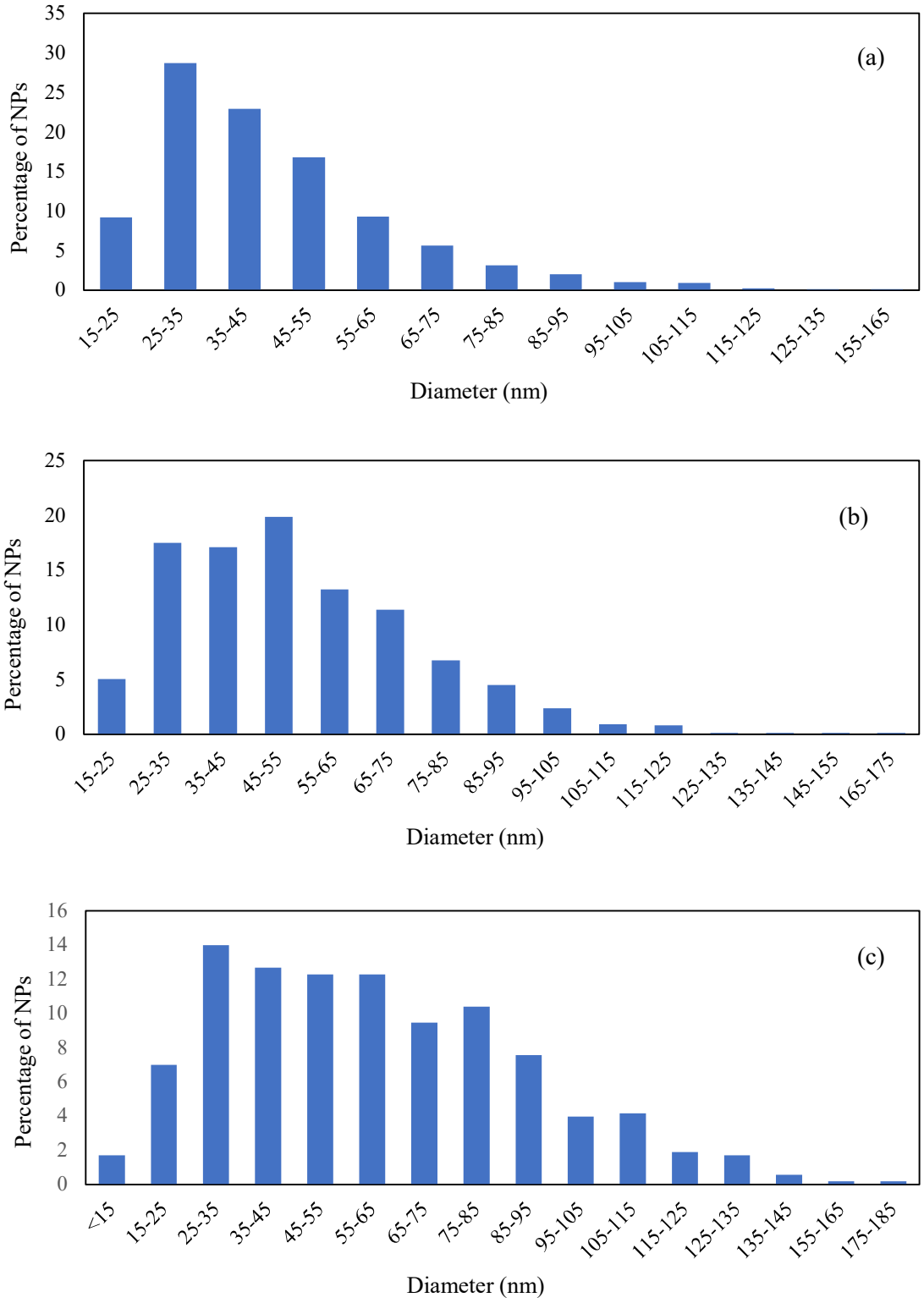

Fig. 4. Histogram of the NP diameter distribution for the samples anodized at (a) room temperature, (b) 40°C and (c) 60°C.

Fig. (5) shows the total number of NPs on a surface area of 2064×2064 nm^2 for the different anodization temperatures. The value of the SD for the number of NPs is also considered here. The total number of NPs on the surface of the samples is decreased as the anodization temperature is increased. This reduction in the total number of NPs on a specified area can be ascribed to the increase in the diameter of the obtained NPs. As can be seen in Fig. (5), the SD value for the total number of NPs decreases from room temperature to 40°C, and then it is increased in the 60°C sample, where the value for the 40°C sample is at minimum. This could be interpreted as the higher regularity of the NPs formed on the 40°C anodized sample.

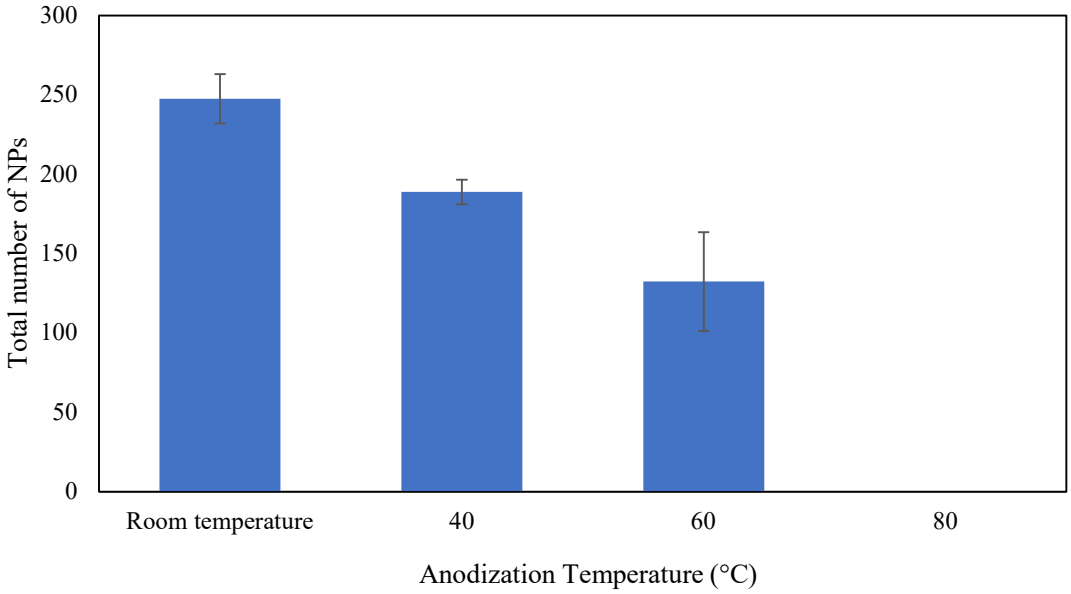

Fig. 5. Total number of NPs formed on the different samples over the surface area of 2064×2064 nm^2.

4- Conclusions

This work investigated the influence of the anodization temperature on the formation and morphology of the resulted NP layer. It was found that the increase in the anodization temperature results in the reduction of the oxide layer thickness. Also, the maximum obtainable thickness for the NP layer (13.7 μm) is possible when the sample is anodized at room temperature. Additionally, it was realized that anodization of NiTi at 80°C results in the complete destruction of the NP layer. Besides, the increase in the electrolyte temperature results in the increase of the mean diameter of NPs. It is eventually concluded that the electrolyte temperature has a deciding role in the morphological characteristics of the resulted nanoporous layer.

References

1. Regonini, D., et al., *A review of growth mechanism, structure and crystallinity of anodized TiO2 nanotubes.* Materials Science and Engineering: R: Reports, 2013. **74**(12): p. 377-406.
2. Hou, G.-Y., et al., *Electrocatalytic performance of Ni-Ti-O nanotube arrays/NiTi alloy electrode annealed under H2 atmosphere for electro-oxidation of methanol.* International Journal of Hydrogen Energy, 2016. **41**(22): p. 9295-9302.
3. He, H., et al., *Ordered NiO–TiO2 nanotube arrays as an efficient catalyst support for methanol oxidation.* Physica Status Solidi (A), 2015. **212**(9): p. 2085-2090.
4. Hang, R., et al., *Highly ordered Ni–Ti–O nanotubes for non-enzymatic glucose detection.* Materials Science and Engineering: C, 2015. **51**: p. 37-42.
5. Li, Z., et al., *Hydrogen sensing with Ni-doped TiO2 nanotubes.* Sensors, 2013. **13**(7): p. 8393-8402.
6. Hang, R., et al., *Preparation, characterization, corrosion behavior and bioactivity of Ni2O3-doped TiO2 nanotubes on NiTi alloy.* Electrochimica Acta, 2012. **70**: p. 382-393.
7. Huan, Z., et al., *Synthesis and characterization of hybrid micro/nano-structured NiTi surfaces by a combination of etching and anodizing.* Nanotechnology, 2014. **25**(5): p. 055602.
8. Roy, P., S. Berger, and P. Schmuki, *TiO2 nanotubes: synthesis and applications.* Angewandte Chemie International Edition, 2011. **50**(13): p. 2904-2939.
9. Davoodian, F., et al., *PLGA-coated drug-loaded nanotubes anodically grown on nitinol.* Materials Science and Engineering: C, 2020: p. 111174.
10. Hang, R., et al., *Fabrication of Ni-Ti-O nanotube arrays by anodization of NiTi alloy and their potential applications.* Scientific Reports, 2014. **4**: p. 7547.
11. Hang, R., et al., *Fabrication of Ni-Ti-O nanoporous film on NiTi alloy in ethylene glycol containing NaCl.* Surface and Coatings Technology, 2017. **321**: p. 136-145.
12. Hang, R., et al., *Anodic growth of ultra-long Ni-Ti-O nanopores.* Electrochemistry Communications, 2016. **71**: p. 28-32.
13. Liu, Y., et al., *Ethylene glycol+ H2O+ Na2CO3: A new electrolyte system to anodically grow Ni-Ti-O nanopores on NiTi alloy.* Materials Letters, 2018. **215**: p. 1-3.

14. Hang, R., et al., *Length-dependent corrosion behavior, Ni2+ release, cytocompatibility, and antibacterial ability of Ni-Ti-O nanopores anodically grown on biomedical NiTi alloy.* Materials Science and Engineering: C, 2018. **89**: p. 1-7.
15. Hang, R., et al., *The influence of electrolyte pH on anodic growth of Ni-Ti-O nanopores on NiTi alloy.* Materials Letters, 2018. **220**: p. 190-193.
16. Liu, Y., et al., *The effects of annealing temperature on corrosion behavior, Ni2+ release, cytocompatibility, and antibacterial ability of Ni-Ti-O nanopores on NiTi alloy.* Surface and Coatings Technology, 2018. **352**: p. 175-181.
17. Strnad, G., et al., *Synthesis of Ti-Ni-O Modified Surfaces on Shape Memory Alloys for Biomedical Applications.* Procedia Manufacturing, 2020. **46**: p. 27-33.
18. Zhao, Y., et al., *The Influence of Electrolyte Stirring on Anodic Growth of Ni-Ti-O Nanopores on NiTi Alloy.* Surface Review and Letters, 2019. **26**(03): p. 1850162.
19. Hang, R., et al., *Electrochemical synthesis, corrosion behavior and cytocompatibility of Ni-Ti-O nanopores on NiTi alloy.* Materials Letters, 2017. **202**: p. 5-8.